Crystalline and Amorphous Phases in the Poly(ethylene oxide)−$LiCF_3SO_3$ System

Roger Frech,*,† Sangramithra Chintapalli,† Peter G. Bruce,‡ and Colin A. Vincent‡

Department of Chemistry and Biochemistry, University of Oklahoma, Norman, Oklahoma 73019, and School of Chemistry, University of St. Andrews, St. Andrews, Fife, KY16 9ST, U.K.

Received August 11, 1998; Revised Manuscript Received November 17, 1998

ABSTRACT: A detailed vibrational spectroscopic study of the ionic species present in the $(PEO)_x$LiTf system ($x = 3-100$) indicates that "free" ions and ion pairs are the dominant species present in the dilute salt region at room temperature. When the salt concentration is increased to an O:M ratio of about 40:1, a band due to an aggregate species first appears and is assigned to the triflate ion vibrating in the $(PEO)_3LiCF_3SO_3$ compound. The amorphous phase of $(PEO)_3LiCF_3SO_3$ was studied by examining the temperature dependence of the spectra as the compound was heated through the melting transition at about 176 °C. Spectral behavior of the CH_2 rocking modes and the COC stretching mode indicated that disordering above the melting temperature resulted in a broad distribution of −O−C−C−O− torsional angles. However the basic lithium-polyether backbone interaction was not been significantly changed for at least 15 °C above the transition temperature. Additional effects of thermal disordering were noted in the CF_3 symmetric stretching mode and the antisymmetric stretching mode, reflecting an increase in the reorientational motion of CF_3 end of the anion. These observations are consistent with the large values of the fluorine atom isotropic temperature factors noted in an X-ray diffraction study. Although the phase diagram reports only two phases present at room temperature (crystalline PEO and the compound $(PEO)_3LiCF_3SO_3$), the spectral data clearly show that there is an additional phase present at intermediate salt concentrations which appears to be an amorphous PEO phase containing dissolved lithium triflate. If only crystalline PEO and the compound are present at equilibrium, the approach to the equilibrium state must be very slow indeed.

1. Introduction

There has been a high degree of scientific interest and a great amount of research in the area of polymer electrolytes,[1] with much of this work focused on poly(ethylene oxide), PEO, and PEO-based polymers into which various salts have been dissolved. Despite these efforts, there has emerged only a very general understanding of the factors which underlie the mechanism of ionic conductivity. The generally accepted picture of ion transport in these polymer-salt systems is that conduction occurs primarily through amorphous regions of the complex,[2,3] with segmental motion of the polymer backbone[4,5] and ionic association[6,7] effects playing a major role. One of the more widely studied systems is PEO complexed with lithium trifluoromethanesulfonate, $LiCF_3SO_3$, which will be abbreviated LiTf. The emphasis on lithium salts reflects the potential application of lithium ion conducting polymer electrolytes in the manufacture of lithium polymer batteries.[8] In addition, the trifluoromethanesulfonate or triflate anion has been of particular interest since the frequencies of certain of its intramolecular vibrational modes are quite sensitive to ionic association. The presence of "free" ions, ion pairs, and more highly associated ionic species can be easily inferred from the vibrational spectrum.[9,10]

Preliminary studies at a few intermediate salt concentrations in the PEO−LiTf system do indeed reveal the presence of "free" ions and ion pairs. However according to the phase diagram,[11] at room temperature there are two phases present, pure crystalline PEO and the compound $(PEO)_3LiCF_3SO_3$. The structure of the compound has been solved by Lightfoot et al. using X-ray diffraction techniques[12] and clearly shows no suggestion of either "free" ions or a structure which might be construed as an ion pair. Therefore a systematic study of the ionic association present in this system as a function of salt concentration is clearly warranted.

Given that the ionic conductivity of this system occurs primarily in the amorphous phase, insight into the structure of the amorphous electrolyte would be particularly important. The availability of the crystal structure from X-ray diffraction measurements suggests a temperature-dependent spectroscopic study of the compound $(PEO)_3LiCF_3SO_3$ through the crystalline phase and into the amorphous phase. We have reported preliminary results of a temperature-dependent spectroscopic study of the $(PEO)_3LiCF_3SO_3$ compound, which focused on the nature of the ionic association in the amorphous phase.[13] In that study it was concluded that the majority ionic species is $[Li_2CF_3SO_3]^+$, which, in the absence of "free" triflate ions, ion pairs, or the triple anion $[Li(CF_3SO_3)_2]^-$, must be present in the amorphous phase as part of an extended ionic chain as in the crystal. However it is useful to further examine the nature of the amorphous phase by monitoring the temperature dependence of a number of spectral regions which reflect cation-polymer interactions.

2. Experimental Section

2.1. Preparation of PEO−Salt Systems. Stoichiometric amounts of PEO and the desired salt were dissolved in acetonitrile and stirred continuously for 24 h at room temperature. The solution was then allowed to stand at room temperature for 24 h to facilitate degassing. To obtain thin films of the samples, the gelatinous polymer solution was cast on a Teflon support. Solvent evaporation led to pinhole free

† University of Oklahoma.
‡ University of St. Andrews.

10.1021/ma9812682 CCC: $18.00
Published on Web 01/21/1999

films of uniform thickness which were then dried in a vacuum oven at ~100 °C for 20 h. The composition of a PEO-salt system is described by the O:M ratio, which is simply the ratio of the number of ether oxygen atoms to the number of cations. It is important to note that at room temperature $(PEO)_xLiCF_3SO_3$ is a heterogeneous system consisting of a pure crystalline PEO phase, the $(PEO)_3LiCF_3SO_3$ compound, and an amorphous PEO phase containing some dissolved lithium triflate. Therefore when a $(PEO)_xLiCF_3SO_3$ composition is reported, the composition refers to the overall sample composition.

2.2. Infrared and Raman Spectroscopy. For infrared measurements, thin films were cast on CsI windows of dimensions 38 mm × 19 mm × 4 mm and dried at ~80 °C for 30 min. The IR transmission spectra were recorded on a Bruker IFS66V FT-IR spectrometer in the region 4000−400 cm^{-1} at a resolution of 2 cm^{-1}. The sample chamber was purged with dry air to exclude the infrared-active H_2O and CO_2 atmospheric bands.

Temperature-dependent spectra were recorded using a specially designed cell which sandwiched the polymer film and a Teflon spacer between two circular windows 19 mm in diameter and 2 mm thick. The sample chamber was purged with nitrogen gas during data acquisition. The temperature was controlled with a Cole-Parmer Digisense temperature controller at an accuracy of ±0.2 °C using a K-type thermocouple. The samples were allowed to equilibrate for an hour at each temperature before data acquisition.

Room temperature Raman spectra were measured with a Jobin Yvon Model T64000 Raman system equipped with a thermoelectrically cooled CCD detector. The thin films, prepared as described earlier, were sandwiched between two glass slides. Spectra were recorded in the triple monochromator mode at a 16 s integration time and 10 accumulations. Excitation was provided by the argon ion laser line at 514.5 nm at a power of 300 mW.

2.3. Differential Scanning Calorimetry Measurements. Differential scanning calorimetry (DSC) data were collected with a Mettler DSC 820 calorimeter. A 4−10 mg sample sealed in a 40 mL aluminum pan was used for each DSC measurement. The DSC scans were recorded from −25 to +275 °C at a 10 K/min heating rate under an N_2 atm whose flow rate was 87 mL/min.

3. Results and Discussion

3.1. Ionic Association as a Function of Salt Concentration. Figure 1 shows spectra for the PEO−$LiCF_3SO_3$ complexes as a function of O:M ratio in the $\nu_s(SO_3)$ spectral region. The band at 1032 cm^{-1} is assigned to "free" triflate ions,[9, 10] the band at 1040 cm^{-1} is assigned to contact ion pairs,[9,10] and the band at 1045 cm^{-1} is usually assigned to the triple ion $[Li_2Tf]^+$.[14,15] These assignments are consistent with an ab initio calculation[12] and a normal coordinate analysis.[16] In the $(PEO)_3LiCF_3SO_3$ compound two oxygen atoms of each triflate anion are in turn each coordinated to a different lithium ion. Consequently each triflate ion vibrates as an $[Li_2Tf]^+$ species. At high salt concentrations in $(PEO)_xLiCF_3SO_3$ with $x > 3$, the band at 1045 cm^{-1} is probably due to the $\nu_s(SO_3)$ mode of the triflate ion in the compound[17] which is expected to be present according to the phase diagram.[11] At lower overall salt concentrations there may exist regions of amorphous PEO in which the concentration of dissolved lithium triflate is sufficiently high such that a local PEO−LiTf structure is present which is very similar to that in the crystalline compound. However it is not possible at this time to spectroscopically distinguish between these two cases.

The spectral resolution of the ion pair band from the band at 1045 cm^{-1} is very difficult without curve-fitting techniques. In the 60:1 and 40:1 complexes it is hard to discern the ion pair band, although in the 20:1 and more concentrated salt complexes the ion pair band appears as a slight asymmetry on the low-frequency side of the broad triple ion band. The shoulder at ~1056 cm^{-1}, visible in the 9:1 and more highly concentrated PEO−LiTf systems, is due to a mixture of COC stretching + CH_2 rocking motion of the compound[18] which is shifted compared to the corresponding mode in pure PEO at 1060 cm^{-1}.

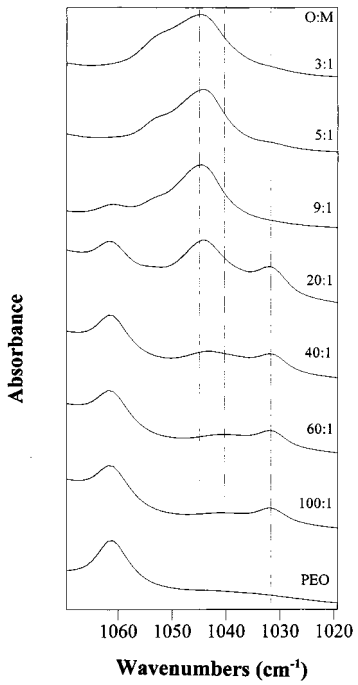

Figure 1. Infrared absorbance spectra of $(PEO)_xLiTf$ in the SO_3 symmetric stretching region. The dashed lines at 1032, 1040, and 1045 cm^{-1} indicate the frequencies of "free" ions, ion pairs, and the 3:1 compound, respectively.

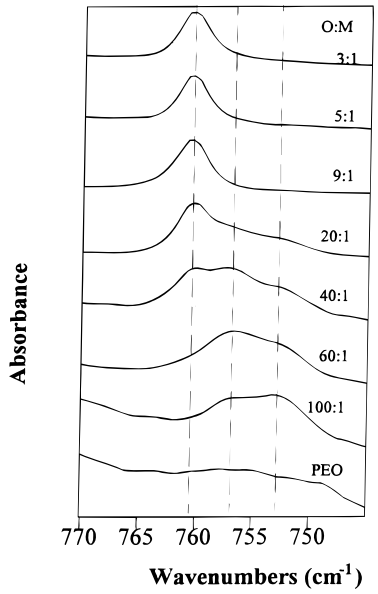

Figure 2. Infrared absorbance spectra of $(PEO)_xLiTf$ in the CF_3 symmetric deformation region. The dashed lines at 753, 757, and 761 cm^{-1} indicate the frequencies of "free" ions, ion pairs, and the 3:1 compound, respectively.

Figure 2 shows the spectra for the $(PEO)_xLiTf$ system as a function of O:M ratio in the $\delta_s(CF_3)$ spectral region. At dilute salt concentrations the "free" ion band at 753 cm^{-1} and the ion pair band at 757 cm^{-1} are easily

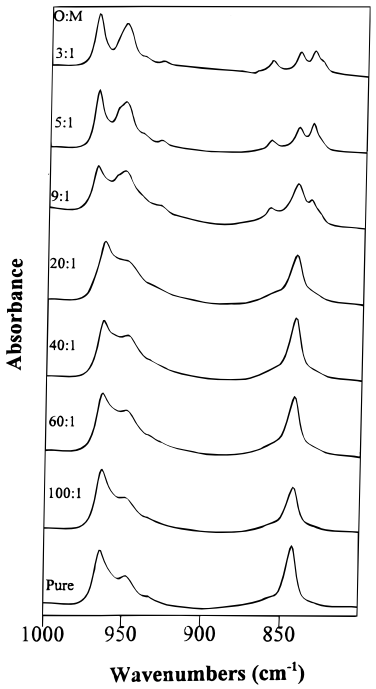

Figure 3. Infrared absorbance spectra of $(PEO)_x LiTf$ in the spectral region from 800 to 1000 cm^{-1}.

distinguished and are indicated by dashed lines which serve as guides in the figure. The "free" ion band is more intense than the ion pair band in the 100:1 system, but these relative intensities are reversed in the 60:1 system. With increasing salt concentration, a band appears at 760 cm^{-1} and grows in intensity until there is only a single band centered at that frequency in the 3:1 system, which is the stoichiometry of the $(PEO)_3$-$LiCF_3SO_3$ compound. The triple ion band first clearly appears in the 40:1 system, as it does in the SO_3 symmetric stretching region. A comparison of Figures 1 and 2 suggests that especially in high molecular weight PEO−LiTf systems, the $\delta_s(CF_3)$ mode may be somewhat more sensitive to the presence of ionic association than is the $\nu_s(SO_3)$ mode.

3.2. Polymer Backbone Conformation. The spectral region 1000−800 cm^{-1} shown in Figure 3 is characteristic of the C−O stretching and CH_2 rocking modes.[19] The spectrum of pure PEO is also shown for comparison. The mode responsible for the band at 844 cm^{-1} is primarily due to the CH_2 rocking motion with a little C−O stretching motion mixed in, while the bands at 964 and 949 cm^{-1} originate primarily in the C−O stretching motion with some contribution from the CH_2 rocking motion. When the salt concentration concentration is increased to 20:1, bands appear at 860, 834, 969, 956 and 952 cm^{-1}. These bands have been ascribed to the compound on the basis of a temperature variation study of a $(PEO)_9LiCF_3SO_3$ system reported earlier.[17] The frequencies of bands primarily due to CH_2 rocking motion are particularly sensitive to the local conformation of the polymer, specifically the O−C−C−O torsional angle.[20,21] The bands at 860 and 834 cm^{-1} are assigned to the CH_2 rocking motion of that portion of the PEO forming the $(PEO)_3LiTf$ compound. The appearance of one mode at a higher frequency and the second mode at a lower frequency than is observed in pure PEO originates in the interaction of the lithium ion with the ether oxygens of the PEO backbone. To coordinate the cation, the O−C−C−O torsional angle decreases in the compound relative to its value in pure PEO. The frequency of the A component of the CH_2 rocking mode increases while the B component decreases frequency with decreasing torsional angle as shown by ab initio calculations.[20]

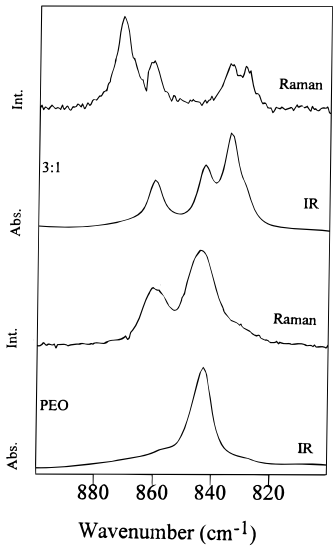

Figure 4. Comparison of infrared absorbance spectra and Raman scattering spectra of pure PEO and the 3:1 compound in the spectral region from 800 to 900 cm^{-1}.

The IR and Raman spectra in the region 800−900 cm^{-1} are compared in Figure 4 for the 3:1 compound and PEO. In the Raman spectrum of pure PEO (the two bottom curves) there two bands at 861 and 846 cm^{-1} which are analogous to the IR-active modes at 857 and 843 cm^{-1}. These observations are consistent with the crystal structure of pure PEO which belongs to the monoclinic space group $P2_1/a$ (C_{2h}^5) and has a center of symmetry. According to the mutual exclusion principle, vibrational modes that are active in a Raman scattering experiment are necessarily inactive in an IR absorption experiment and vice versa. Similar infrared/Raman exclusion behavior is observed in the IR and Raman spectra of crystalline $(PEO)_3LiCF_3SO_3$ (two top curves), as its space group is also $P2_1/a$ (C_{2h}^5). The Raman-active modes are seen at 871, 861, 834, and 829 cm^{-1}, with the IR-active modes at 860, 844, and 834 cm^{-1}.

3.3. CH_2 Twisting Modes and SO_3 Antisymmetric Stretching Mode. Figure 5 shows the IR spectra in the region 1320−1220 cm^{-1}. The peaks at 1236, 1244, and 1280 cm^{-1} are due to the CH_2 twisting modes in pure PEO. These peaks decrease in intensity with increasing $LiCF_3SO_3$ concentration, and are replaced by corresponding peaks due to the CH_2 twisting modes in the 3:1 compound. Although there is very little frequency shift of these modes between pure PEO and the compound, there are significant intensity differences as is evident in the spectra, particularly in the modes at 1236 and 1280 cm^{-1}.

At very dilute concentrations, the $\nu_s(CF_3)$ mode for a "free" ion is visible at 1224 cm^{-1}. The corresponding ion pair band appears at 1226 cm^{-1} in the 60:1 complex. With an increase in the salt concentration, this peak shifts to higher frequency, and in the 3:1 compound there is only a single band at 1233 cm^{-1}.

The doubly degenerate $\nu_{as}(SO_3)$ mode is also useful to examine cation−anion interactions in these systems.[21] This band appears at 1275 cm^{-1} for the "free" ion and is masked due to the presence of the crystalline

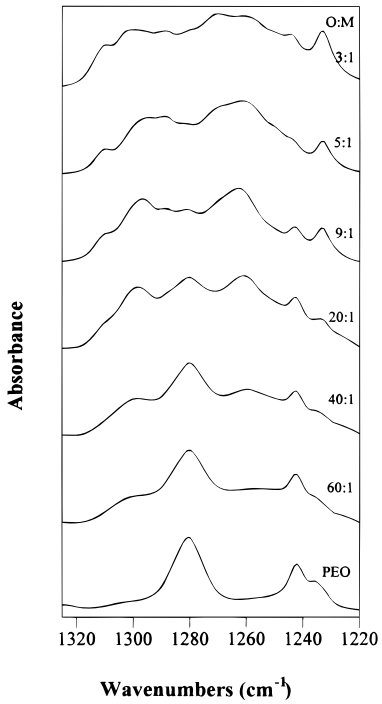

Figure 5. Infrared absorbance spectra of $(PEO)_x$LiTf in the spectral region from 1220 to 1320 cm^{-1}.

PEO peak. However with an increase in salt concentration, ion pairs form and the degeneracy is lifted by the cation interaction. Consequently the $\nu_{as}(SO_3)$ band splits into two bands at 1265 and 1298 cm^{-1}, which begin to appear in the 20:1 complex. At a 9:1 salt concentration there is a subtle frequency shift of the two components to 1263 and 1297 cm^{-1} as the 3:1 compound becomes the dominant species in the spectrum. A close examination of the spectra of the more highly concentrated systems O:M = 9:1 shows two additional bands at 1288 and 1281 cm^{-1} in this region. These are attributed to factor group components of the $\nu_{as}(SO_3)$ mode.

3.4. Thermal Data. Several representative DSC thermograms are shown in Figure 6. In the 20:1 composition, the strong, sharp melting transition of crystalline PEO is seen slightly below 60 °C, with the broad transition between 100 and 140 °C due to the compound. In the 9:1 composition, the melting transition of the crystalline PEO is still observed, and the crystalline-to-amorphous phase transition of the compound is considerably narrower and higher in temperature. At 5:1 there is only the transition of the compound visible, and at 3:1 the onset of the melting transition is at 176 °C. The overall behavior of the DSC data is that expected in two component system exhibiting a eutectic point.

3.5. Nature of the Amorphous $(PEO)_3LiCF_3SO_3$ Compound. The vibrational spectra of the $(PEO)_x$-$LiCF_3SO_3$ system have been examined in the first three sections, with particular emphasis on the compound $(PEO)_3LiCF_3SO_3$. As noted in the Introduction, we have previously described a brief study of ionic association in the compound as function of temperature. To briefly summarize, neither the frequency of the $\nu_s(SO_3)$ mode at 1046 cm^{-1} nor that of the $\delta_s(CF_3)$ band at 760 cm^{-1} changes with increasing temperature up to the onset of melting, although thermal broadening of the bands is apparent. Above the melting point there are broad features at 1046 and 763 cm^{-1} which correspond

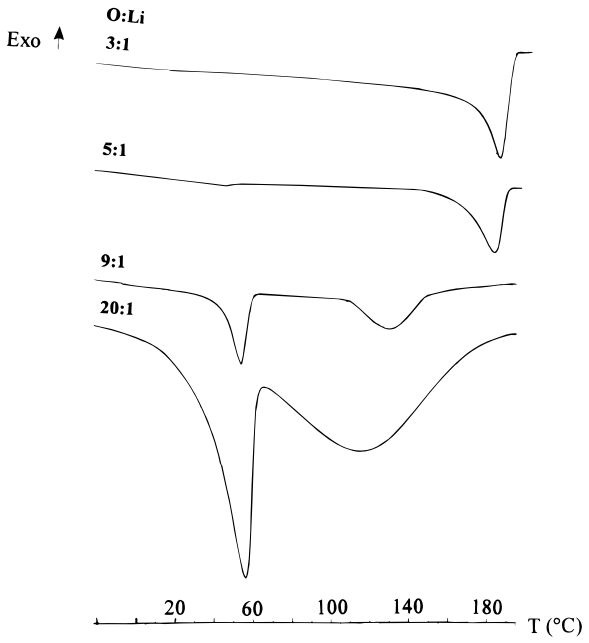

Figure 6. Differential scanning calorimetry thermograms of $(PEO)_x$LiTf for x = 20, 9, 5, and 3.

to the frequencies of an $[Li_2CF_3SO_3]^+$ species. These bands cannot be attributed to individual, isolated $[Li_2CF_3SO_3]^+$ triple ions as recognized in the oligomer-lithium triflate solutions. The presence of individual triple ions necessarily requires the presence of "free" $CF_3SO_3^-$ or the $[Li(CF_3SO_3)_2]^-$ species due to charge balance considerations; however, a detailed spectroscopic study rules out this possibility. It was therefore concluded that the majority species is $[Li_2CF_3SO_3]^+$ which in the absence of $CF_3SO_3^-$ or $[Li(CF_3SO_3)_2]^-$ must be present in the amorphous phase as part of an extended ionic chain as in the crystal.

Further insight into the nature of the amorphous phase of $(PEO)_3LiCF_3SO_3$ can be obtained by examining the temperature dependence of the modes in the spectral region 1000−800 cm^{-1}, which are sensitive to the local conformation of the PEO backbone. Figure 7 shows the spectra for the 3:1 compound as a function of temperature in this region. The frequencies of the three CH_2 rocking bands at 860, 843 and 834 cm^{-1} remain unshifted, and no new bands appear as the crystalline phase is heated to the melting point. Although some thermal broadening occurs, the three bands are easily distinguishable at 173 °C. At 176 °C there is a marked increase in the broadening, and at 180 °C there is only a single broad peak. The simplest interpretation of these data is that in the amorphous phase there a broad distribution of −O−C−C−O− torsional angles, as the regular conformations which characterize the crystalline phase become disordered. It is important to note, however, that there is no major shift in the frequency of these modes between the highest temperature (176 °C) at which the spectrum of the crystalline phase is recorded and the spectrum of the amorphous phase (180 °C), suggesting that the basic lithium−polyether backbone interaction has not been significantly altered upon melting of the crystals.

This conclusion is underscored by the behavior of the COC stretching mode which provides further insight into the cation−polymer interactions. Figure 8 compares this mode in pure PEO and the 3:1 complex at 190 °C. The frequency shift from 1112 cm^{-1} in PEO to 1081

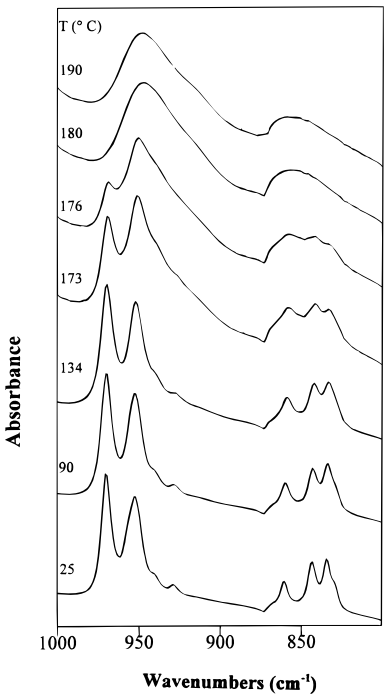

Figure 7. Infrared absorbance spectra of the 3:1 compound in the spectral region from 800 to 1000 cm^{-1} over the temperature range from 25 to 190 °C.

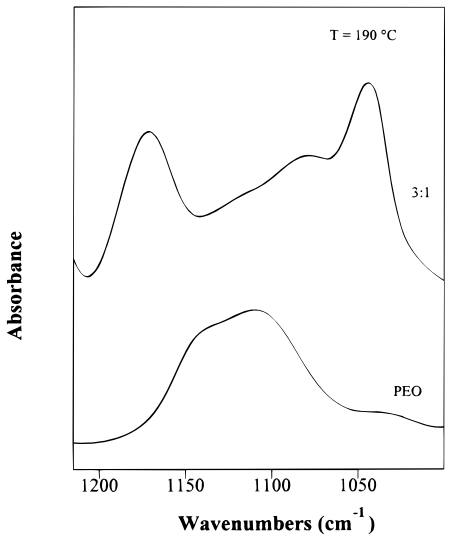

Figure 8. A comparison of the infrared absorbance spectrum of pure PEO and the 3:1 compound in the spectral region from 1000 to 1200 cm^{-1} at 190 °C.

cm^{-1} in the compound is clear evidence for a strong lithium−polyether oxygen interaction in the amorphous phase. The bands at 1170 and 1046 cm^{-1} in the spectrum of the 3:1 complex are due to $\nu_{as}(CF_3)$ and $\nu_s(SO_3)$ respectively and can be ignored for this comparison.

The temperature variation study of the 3:1 complex shows that the structure of the amorphous phase is very similar to that of the crystalline complex, with only a loss of long range order arising from a loss of register between adjacent PEO chains and some disordering in the helical torsion angles. In the amorphous phase for at least 15 °C above the melting transition, the PEO chains remain helical with each turn of the helix containing a Li^+ which has the same coordination to the ether oxygens as in the crystalline phase. Also, the

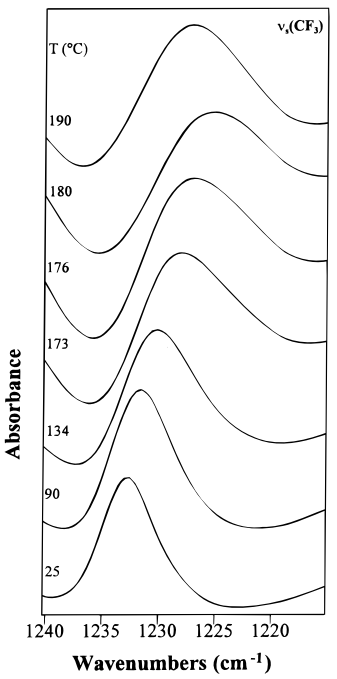

Figure 9. Infrared absorbance spectra of the 3:1 compound in the CF_3 symmetric stretching region over the temperature range from 25 to 190 °C.

$CF_3SO_3^-$ ions continue to bridge neighboring Li^+ ions along the chains forming a zigzag arrangement $Li^+-CF_3SO_3-Li^+$. Consequently there is a unique set of cations and anions associated with each chain.

The spectroscopic study also indicates a subtle structural or dynamical change in the anion with increasing temperature, primarily involving the CF_3 end. Figure 9 shows the CF_3 symmetric stretching mode, $\nu_s(CF_3)$, as a function of temperature. There is a gradual decrease in the frequency of the mode over the entire temperature range studied, from 1233 cm^{-1} at 28 °C to 1228 cm^{-1} at 190 °C. Between 176 and 180 °C there is a transition into the completely amorphous phase, as evidenced by the increased broadening of the band. It is important to compare this behavior with that of the SO_3 end of the anion. The spectra of the SO_3 symmetric stretching mode, $\nu_s(SO_3)$, show a smaller frequency decrease (1 cm^{-1}) followed by the expected increase in bandwidth in the amorphous phase.

Figure 10 shows the temperature dependence of the CF_3 antisymmetric stretching mode, $\nu_{as}(CF_3)$. In these spectra there is only a slight decrease in the frequency up to 176 °C, and then a marked decrease accompanied by a dramatic broadening of the band. It is necessary to consider why the frequency of the $\nu_s(CF_3)$ mode is significantly more temperature-dependent than that of $\nu_{as}(CF_3)$ or $\nu_s(SO_3)$. We postulate that the temperature dependence of these modes originates in an increase in the degree of reorientational motion of the CF_3 end of the anion. According to the crystal structure of the compound, the SO_3 groups are coordinated to lithium ions which are in turn coordinated to the oxygen atoms of the polyether backbone. However the CF_3 groups are essentially "free" in that their interactions with each other and with other nearby atoms are through weak van der Waals forces. A group frequency such as that of the $\nu_s(CF_3)$ mode depends, inter alia, on the potential energy environment of the CF_3 group. Although this frequency can reflect local structural details, this fre-

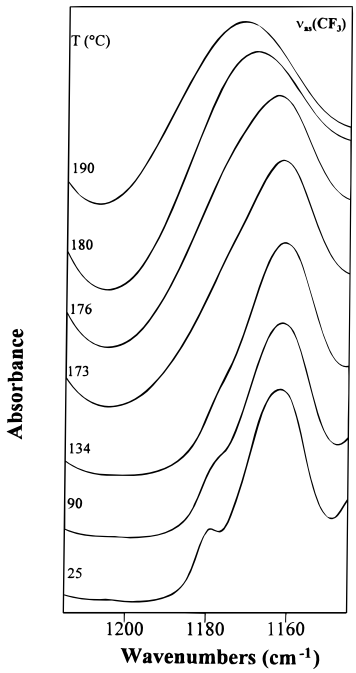

Figure 10. Infrared absorbance spectra of the 3:1 compound in the CF_3 antisymmetric stretching region over the temperature range from 25 to 190 °C.

quency also reflects the local density about the CF_3 group. In general, the frequency of a symmetric stretching mode is more sensitive to the local density about the vibrating species than is the corresponding antisymmetric stretching mode. With the onset of reorientational motion, each CF_3 group attempts to minimize its repulsive interactions with the neighboring CF_3 groups, thereby minimizing its local density. It is important to note that there is a marked *decrease* in the frequency of the $\nu_s(CF_3)$ mode with increasing temperature. In the structure solution of $(PEO)_3LiCF_3SO_3$, the authors describe large values of the isotropic temperature factors, particularly for the fluorine atoms.[12] The relatively smooth variation of these factors as a function of temperature led the authors to conclude that these high values originated in thermal rather than static disorder. This conclusion is consistent with the postulate that the frequency shift seen in Figure 9 originates in changes in the potential energy environment of the CF_3 groups, probably induced by the onset of reorientational motion of those groups, and not in subtle structural changes at the SO_3 end of the anion.

4. Conclusions

Although the phase diagram reports only two phases present at room temperature (crystalline PEO and the compound $(PEO)_3LiCF_3SO_3$), the spectral data clearly show that there is an additional phase present at intermediate concentrations which appears to be an amorphous PEO phase containing dissolved lithium triflate. This is especially evident in Figures 1 and 2 which show bands resulting from "free" ions at low salt concentrations and ion pairs at higher salt concentrations. It should be noted that the relative intensities of these bands, and therefore the relative concentrations of the "free" ions and ion pairs, do not change over a period of several days. If indeed only crystalline PEO and the compound are present at equilibrium, the approach to the equilibrium state must be very slow indeed.

The temperature-dependent vibrational spectra of the $(PEO)_3LiCF_3SO_3$ compound provides useful insight into the nature of the amorphous polymer electrolyte. At 176 °C the compound melts, and above this temperature the system is completely amorphous according to the X-ray data. Spectra of the CH_2 rocking spectral region indicates that the regular TGT−TGT−TG′T conformation present in the compound at room temperature is lost above 176 °C, leaving only a broad distribution of −O−C−C−O− torsional angles. For a range of at least 14 °C above the melting temperature, the lithium ions appear to interact with the polymer backbone much as is observed at room temperature and the interval up to the melting temperature.

Another form of thermal disordering is seen in the spectra of the CF_3 stretching modes, reflecting an increase in the reorientational motion of CF_3 end of the anion. These observations are consistent with the large values of the fluorine atom isotropic temperature factors noted in the X-ray diffraction study of this system.

Acknowledgment. This work was partially supported by funds from the U.S. Army Research Office (Grant No. DAAH04-94-G-0250) and the NSF EPSCoR program (Cooperative Agreement No. OSR-9550478).

References and Notes

(1) Fenton, D. E.; Parker, J. M.; Wright, P. V. *Polymer* **1973**, *7*, 319.
(2) Berthier, C.; Gorecki, W.; Minier, M.; Armand, M. B.; Chabagno, J. M.; Rigoud, P. *Solid State Ionics* **1983**, *11*, 91.
(3) Papke, B. L.; Ratner, M. A.; Shriver, D. F. *J. Electrochem. Soc.* **1982**, *129*, 1694.
(4) Druger, S. D.; Ratner, M. A.; Nitzan, A. *Solid State Ionics* **1983**, *9 & 10*, 1115.
(5) Druger, S. D.; Ratner, M. A.; Nitzan, A. *J. Chem. Phys.* **1983**, *79*, 3133.
(6) Papke, B. L.; Dupon, R.; Ratner, M. A.; Shriver, D. F. *Solid State Ionics* **1981**, *5*, 685.
(7) Watanable, W.; Itoh, M.; Nanui, K.; Ogata, N. *Macromolecules* **1987**, *20*, 669.
(8) Gauthier, M.; Belanger, A.; Kapfer, B.; Vassort, G. In *Polymer Electrolyte Reviews-2*; MacCallum, J. R., Vincent, C. A., Eds.; Elsevier: London, 1989; Chapter 9.
(9) Schantz, S.; Sandahl, J.; Borjesson, L.; Torell, L. M.; Stevens, J. R. *Solid State Ionics* **1988**, *28−30*, 1047.
(10) Schantz, S.; Torell, L. M.; Stevens, J. R. *J. Appl. Phys.* **1988**, *64*, 2038.
(11) Robitaille, C. D.; Fauteux, D. *J. Electrochem. Soc.* **1986**, *133*, 315.
(12) Lightfoot, P.; Mehta, M. A.; Bruce, P. G. *Science* **1993**, *262*, 883.
(13) Frech, R.; Chintapalli, S.; Bruce, P. G.; Vincent, C. A. *Chem. Commun.* **1997**, 157.
(14) Stevens, J. R.; Jaccobssen, P. *Can. J. Chem.* **1991**, *69*, 1980.
(15) Huang, W.; Frech, R.; Wheeler, R. A. *J. Phys. Chem.* **1994**, *98*, 100.
(16) Huang, W.; Frech, R.; Wheeler, R. A. *Spectrochim. Acta* **1994**, *50A*, 985.
(17) Dissanayake, M. A. K. L.; Frech, R. *Macromolecules* **1995**, *28*, 5312.
(18) Yoshihara, T.; Tadokora, H.; Murahashi, S. *J. Chem. Phys* **1964**, 41, 2902.
(19) Matsuura, H.; Fukuhara, K. *J. Polym. Sci., Part B* **1986**, 24, 1383.
(20) Murcko, M. A.; DiPaola, R. A. *J. Am. Chem. Soc.* **1992**, *114*, 10010.
(21) Bernson, A.; Lindgren, J. *Polymer* **1994**, *35*, 4842.

MA9812682